Observation of Asymmetric Stark Profiles from Plasmas Created by a Picosecond KrF Laser

PPPL--2484

DE88 003449

C.H. Nam, W. Tighe, and S. Suckewer
Plasma Physics Laboratory, Princeton University
Princeton, N.J. 08544

J.F. Seely and U. Feldman
E.O. Hulbert Center for Space Research, Naval Research Laboratory
Washington, D.C. 20375

L.A. Woltz
Center for Radiation Research, National Bureau of Standards
Gaithersburg, MD 20899

ABSTRACT

High-resolution extreme ultraviolet (XUV) spectra from solid targets irradiated by a picosecond KrF* laser focused to 10^{16} W/cm^2 have been recorded. The line profiles of transitions in Li-like fluorine and oxygen are asymmetric and up to 2 Å in width. Calculations indicate the presence of transitions of the type 2p-3p and other forbidden Stark components.

Highly charged ions produced by focusing picosecond-duration laser pulses onto gaseous targets have been reported.[1,2] In this letter, we present the first high-resolution XUV spectra obtained by the interaction of powerful picosecond laser pulses with solid targets. The targets were composed of elements with atomic numbers in the range Z = 3 to Z = 26 and were irradiated using a KrF* laser with a pulse duration of 1.2 picosecond and focused to an intensity of 10^{16} W/cm^2. The spectra in the range 6 Å to 370 Å were recorded by a 3 m grazing incidence spectrograph[3] with a resolving power sufficient to observe the line profiles of transitions in highly charged ions.

Picosecond and sub-picosecond laser pulses with power 20-30 GW and focused power density 10^{16} - 10^{17} W/cm^2 (and larger in the near future) can be used to study ions in extremely high electromagnetic fields. The electric field in the laser focus is comparable to the Coulomb field that binds the electrons to the nucleus, and expected processes include the shift of atomic energy levels and spectral line broadening, the generation of intense XUV and X-ray radiation, and multiphoton processes.

The KrF* laser used in the present experiment is part of a larger system which is being constructed for the development of short wavelength X-ray lasers and which includes a CO_2 laser (1 kJ energy, 10-30 nsec pulse duration).[4] A detailed description of this system will be published elsewhere. A schematic of the present experiment is shown in Fig. 1. The master oscillator was a cavity-dumped dye laser tuned to a wavelength of 648 nm. The dye laser used a hybrid mode-locking scheme and produced 1 psec pulses. The dye laser was pumped by the frequency-doubled output of a mode-locked YAG laser. The output of the dye laser was injected into a three-stage dye amplifier that was pumped by amplified, frequency-doubled pulses from the YAG laser. The amplified 648 nm pulses were frequency-doubled and were mixed with 1064 nm YAG pulses. The resulting 248 nm pulses were injected into two KrF* amplifiers. The amplified pulses typically had an energy of 20 to 25 mJ and a duration of 1 to 1.2 psec. The pulses were focused by an f/5 spherical lens to an intensity of approximately 10^{16} W/cm^2. The focus was optimized by observing the signal from an X-ray diode and by examining the crater size using a microscope.

The laser pulses were incident on a cylindrical target at an angle of 30° to the target normal. The spectrograph viewed the focal spot at an angle of 60 ° to the target

normal, and the entrance slit of the spectrograph was 20 cm from the target. The spectra were recorded on Kodak 101 photographic plates, and the spectra produced by up to 7000 laser shots were integrated onto each exposure. The target was rotated to a new position before each laser shot.

The targets were either composed or else coated with the material under study. The spectrum from a solid aluminum target is shown in Fig. 2. Isolated aluminum transitions from low stages of ionization, such as the Ne-like n = 2-3 transitions, were observed to have line widths less than 100 mÅ. These transitions occur in the low-density expansion plasma, and the line widths of these transitions are consistent with the 30 mÅ instrumental broadening (resulting from the 10 μm entrance slit) and Doppler source broadening. The much larger widths of the Li-like n = 2 - 4 and n = 2 - 5 transitions shown in Fig. 2 are consistent with quasi-static ion Stark broadening at an electron density in the range 10^{21} - 10^{22} cm^{-3}. The same transitions in Li-like fluorine from a teflon target are shown in Fig. 3. These line profiles are asymmetric and are up to 2 Å in width. Similar line profiles were observed for Li-like oxygen from a nylon target. Compared to the widths of the aluminum transitions, the Stark widths of the fluorine and oxygen transitions are larger owing to the smaller atomic number of these elements and the longer wavelengths of the transitions.

It is well known that the microfield due to the plasma can cause shifts of the energy levels of emitting ions.[5] In dense plasmas, when the shifts become comparable to the energy level splittings, the wave functions of neighboring states become mixed, and this permits transitions that are not allowed in the absence of the microfield. The parity selection rule breaks down, and normally forbidden transitions between states with the same parity are possible. The ratio of the intensities of the forbidden and allowed transitions increases with plasma density.

Forbidden Stark components have long been observed in neutral emitters.[6] We now show that the asymmetric profiles of the Li-like F^{6+} transitions observed in the present experiment result from forbidden components. The energy levels and wavelenghts[7] for F^{6+} are shown in Fig. 4. The predicted wavelengths of the forbidden 2p-3p transitions (129.385 Å and 129.504 Å) are slightly longer than the wavelengths of

the allowed 2p-3d transitions (127.656 Å and 127.806 Å), and the forbidden component appears as a feature on the red wing of the allowed component.

The line profiles were modeled using a formalism developed for the calculation of spectral line profiles of multielectron ions in dense plasmas.[8] The calculation was done using the quasi-static ion approximation in which the plasma ions that perturb the emitting ion are assumed to have negligible motion during the lifetime of the excited state. A quantum mechanical relaxation theory was used to calculate the plasma electron broadening of the spectral lines. The atomic energy levels and radial matrix elements were calculated using the atomic structure program of Cowan.[9] The microfield probability distributions were calculated using the programs of Tighe and Hooper.[10] The excited levels were assumed to have Boltzmann populations.

The calculated profile of the F^{6+} 2p-3d spectral feature is shown in Fig. 5. At electron densities greater than 5×10^{21} cm^{-3}, the 2p-3p forbidden component contributes significantly to the red wing of the spectral feature. This is consistent with the enhanced red wing of the observed 2p-3d spectral feature shown in Fig. 3. Similarly, the red wing of the observed 2p-4d feature is enhanced by the 2p-4p forbidden component. The calculated line profiles are weak functions of electron temperature.

The line width and asymmetry of the observed F^{6+} 2p-3d spectral feature are consistent with an electron density of approximately 10^{22} cm^{-3}. This density is comparable to the critical electron density (2×10^{22} cm^{-3}) for 248 nm laser radiation and is much smaller than the target density (4×10^{23} cm^{-3}). Since the plasma expansion during the picosecond laser pulse is negligible, it is likely that the observed emission occurs in the expanding plasma immediately after the laser pulse. During this time, the ion microfield is an order of magnitude weaker than the oscillating field of the laser beam (3×10^{9} V/cm) that exists during the laser pulse, and the contribution of the ion microfield to the time-integrated line broadening is apparently dominant owing to its longer duration.

The consideration of the times required for electron collisional ionization and radiative decay also indicates that the broad line emission occurs immediately after the laser pulse. For an electron density of 10^{22} cm^{-3}, the time for the electron energy distribution to relax to a Maxwellian is much less than a picosecond. The time for

collisional ionization to F^{6+} is approximately 1 psec, and the time for n = 2 -3 collisional excitation is less than a picosecond.[11] The times for the radiative transitions 3p-2s and 3d-2p are 20 psec and 6 psec, respectively, and are much larger than the laser pulse duration. Thus the excited F^{6+} ions are formed during the picosecond laser pulse, and the bulk of the emission occurs after the laser pulse. The F^{5+} ionization energy is 160 eV and the F^{6+} n = 2-3 excitation energy is 100 eV, and it is possible that multiphoton (nonresonance) processes, requiring a large number of 248 nm (5 eV) photons, contribute to the formation of excited F^{6+} during the laser pulse.

The spectrum from an iron target is shown in Fig. 6. The surface of this target was contaminated with sodium, and the Li-like sodium lines were observed to be narrow. A target coated with 1500 Å of LiF was also irradiated, and the F^{6+} lines from the coating were observed to be narrow. This implies that the broad Li-like fluorine lines observed from solid targets do not originate in such a thin surface layer. A thin surface layer of target material may be evaporated by a weak prepulse of amplified spontaneous emission (ASE), and the role of the ASE prepulse will be the subject of future work using layered targets. We also note in Fig. 6 the presence of Na-like Fe^{15+} lines, and this represents the most highly charged ion produced in plasmas created by a picosecond laser. The He-like $1s^2\ ^1S_0$ - $1s2p\ ^1P_1$ resonance line of aluminum at 7.757 Å (1.6 keV excitation energy) was identified in the spectra from the aluminum targets.

For electron densities greater than 10^{21} cm^{-3}, the populations of the excited levels of F^{6+} are in Boltzmann equilibrium. In an optically thin plasma, the intensity of the F^{6+} 2p-3d transition is expected to be a factor of five greater than the intensity of the 2s-2p transition, yet the observed peak intensities of the two spectral features are comparable. The 2p-3d transition has the larger oscillator strength and optical depth, and the reduced peak intensity of the 2p-3d feature may result from the opacity at the line center of the 2p-3d transition. The time-dependent calculation of the ionization dynamics and radiation transfer in dense plasmas created by picosecond laser pulses is needed.

In conclusion, the output of a high power picosecond laser (PP-laser) system has been focused onto several solid targets and the interaction has been examined with a high resolution XUV spectrometer. Conditions resulting in significant line broadening and high levels of ionization were observed. Calculations of stark broadening indicate

that the broad line emission occurs immediately after the laser pulse. Experiments involving new targets and detectors and the development of a final stage for the PP-laser to provide still higher power levels are proceeding.

Acknowledgements

We thank C.F. Hooper for suggesting the calculation of the Stark profiles and H. Furth, V.L. Jacobs, R. Kulsrud, M. Littman, R. Miles, T. McIlrath, and E. Valeo for helpful discussions. We also thank W.E. Behring, C.M. Brown, J. Houston, and J. Robinson for assisting with the experiment. This work was supported by the U.S. DOE Advanced Energy Project of Basic Engineering Sciences, contract KC-05-01 (Princeton), and by the Office of Naval Research and SDIO, contract N0001487 (NRL).

References

1. T.S. Luk et al., Phys. Rev. Lett., 51, 110 (1983).
2. A. L'Huillier et al., Phys. Rev. Lett., 48, 1814 (1982).
3. W.E. Behring, R.J. Ugiansky, and U. Feldman, Appl. Optics, 12, 528 (1973).
4. S. Suckewer et al., J. de Phys., 47, C6-23 (1986).
5. H.R. Griem, Spectral Line Broadening by Plasmas (Academic Press, New York, 1974).
6. H.R. Griem, Astrophys. J., 154, 1111 (1968).
7. L.A. Vainshtein and U.I. Safronova, Phys. Scripta, 31, 519 (1985).
8. L.A. Woltz and C.F. Hooper, to be pulished in Phys. Rev. A. (1987).
9. R.D. Cowan, The Theory of Atomic Structure and Spectra (University of Chicago Press, Berkeley, 1981).
10. R.J. Tighe, and C.F. Hooper, Phys. Rev. A., 14, 1514 (1976).
11. I.I. Sobelman, L.A. Vainshtein, and E.A. Yukov, Excitation of Atoms and Broadening of Spectral Lines (Springer-Verlag, New York, 1981), p. 218.

Figure Captions

Fig. 1 Schematic of the experiment.

Fig. 2 Densitometer trace of the spectrum from an aluminum target showing transitions in Li-like AlXI and Be-like AlX. A photograph of the spectrum is shown below the densitometer trace.

Fig. 3 Densitometer trace of the spectrum from a teflon target showing transitions in Li-like FVII and Be-like FVI.

Fig. 4 Wavelengths in Å for the F^{6+} allowed transitions (solid lines) and the 2p-3p forbidden transitions (dashed line).

Fig. 5 Calculated F^{6+} Stark profiles for an electron temperature of 500 eV and electron densities of (a) 2×10^{21} cm^{-3}, (b) 5×10^{21} cm^{-3}, and (c) 1×10^{22} cm^{-3}. The 2p-3p forbidden component appears at 129 Å.

Fig. 6 Densitometer trace of the spectrum of an iron target with surface contamination of sodium. Identified are transitions in Li-like NaIX, Na-like FeXVI, and Mg-like FeXV.

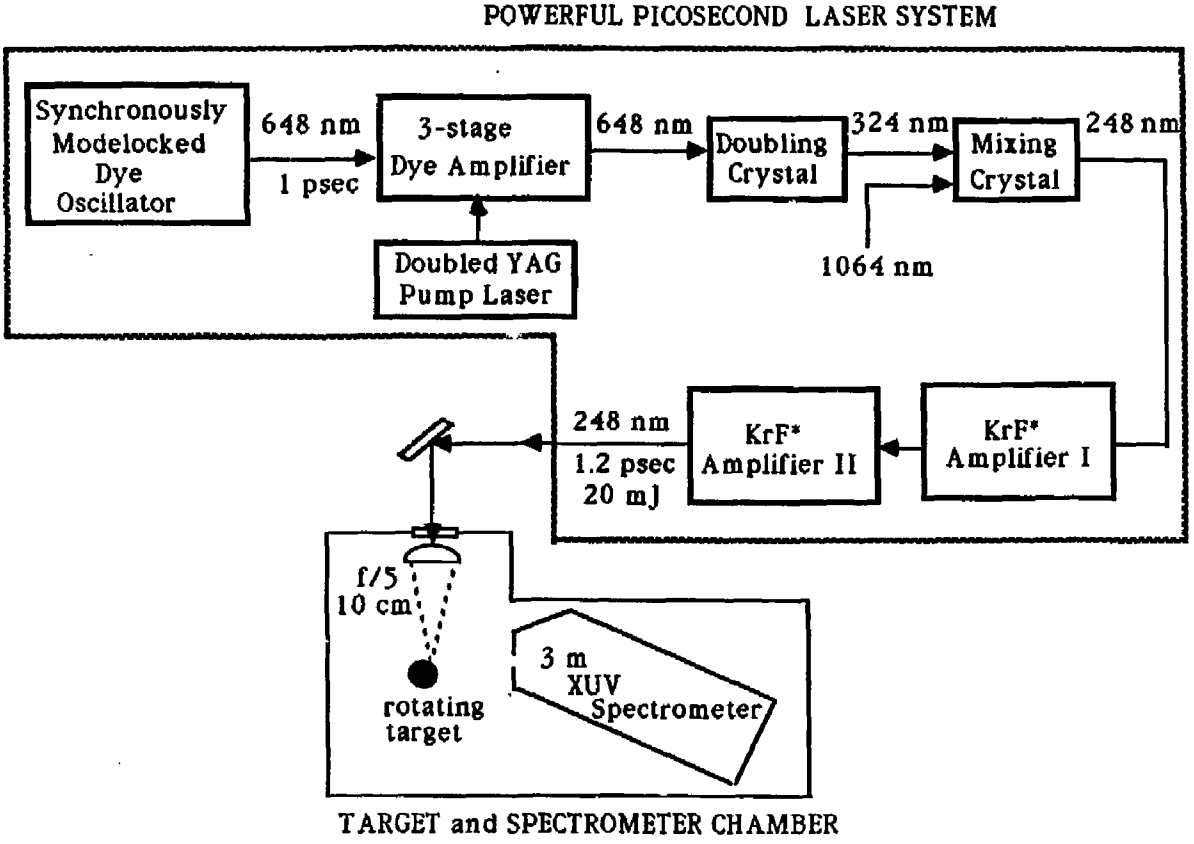

EXPERIMENTAL LAYOUT

Fig. 1

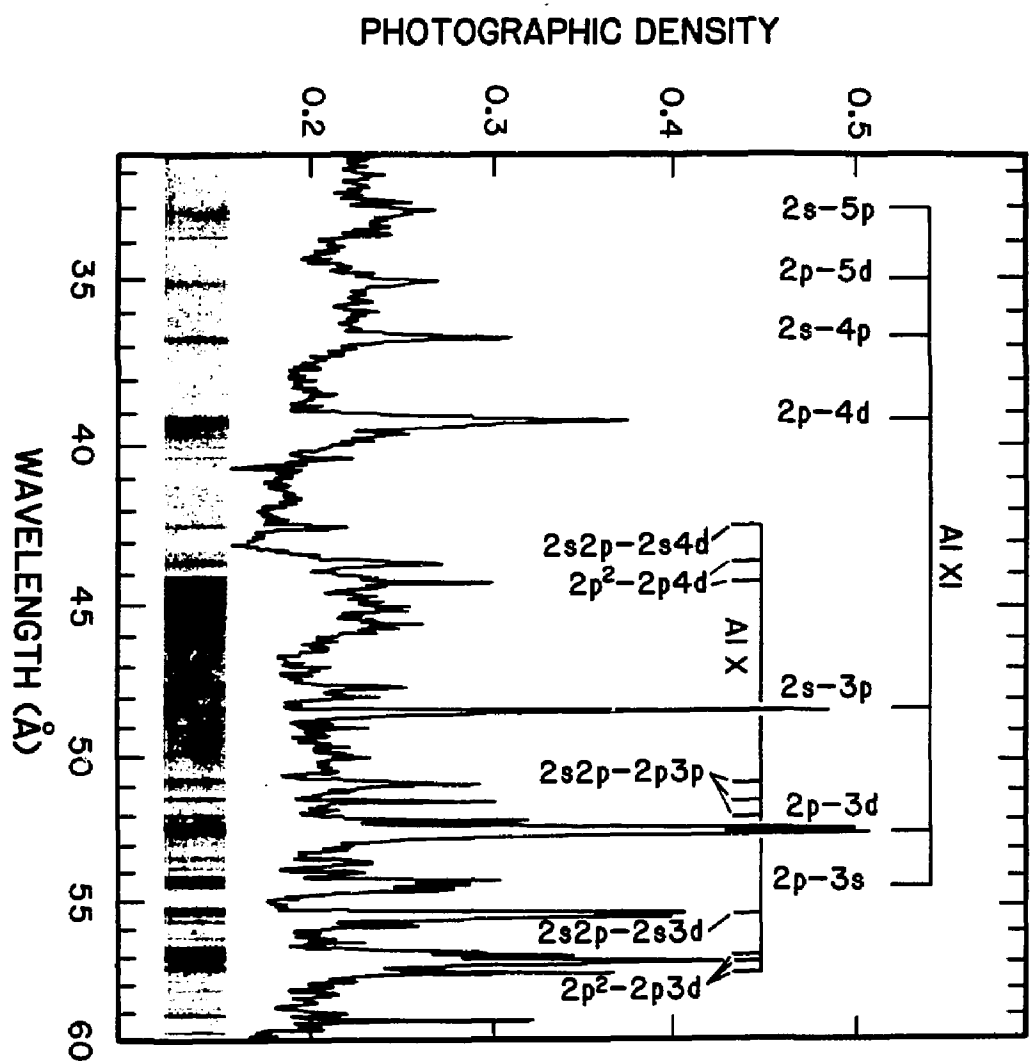
PHOTOGRAPHIC DENSITY
0.2
0.3
0.4
0.5
WAVELENGTH (Å)
35
40
45
50
55
60
2s-5p
2p-5d
2s-4p
2p-4d
2s2p-2s4d
2p²-2p4d
Al X
2s-3p
2s2p-2p3p
2p-3d
2p-3s
2s2p-2s3d
2p²-2p3d
Al XI

Fig. 2

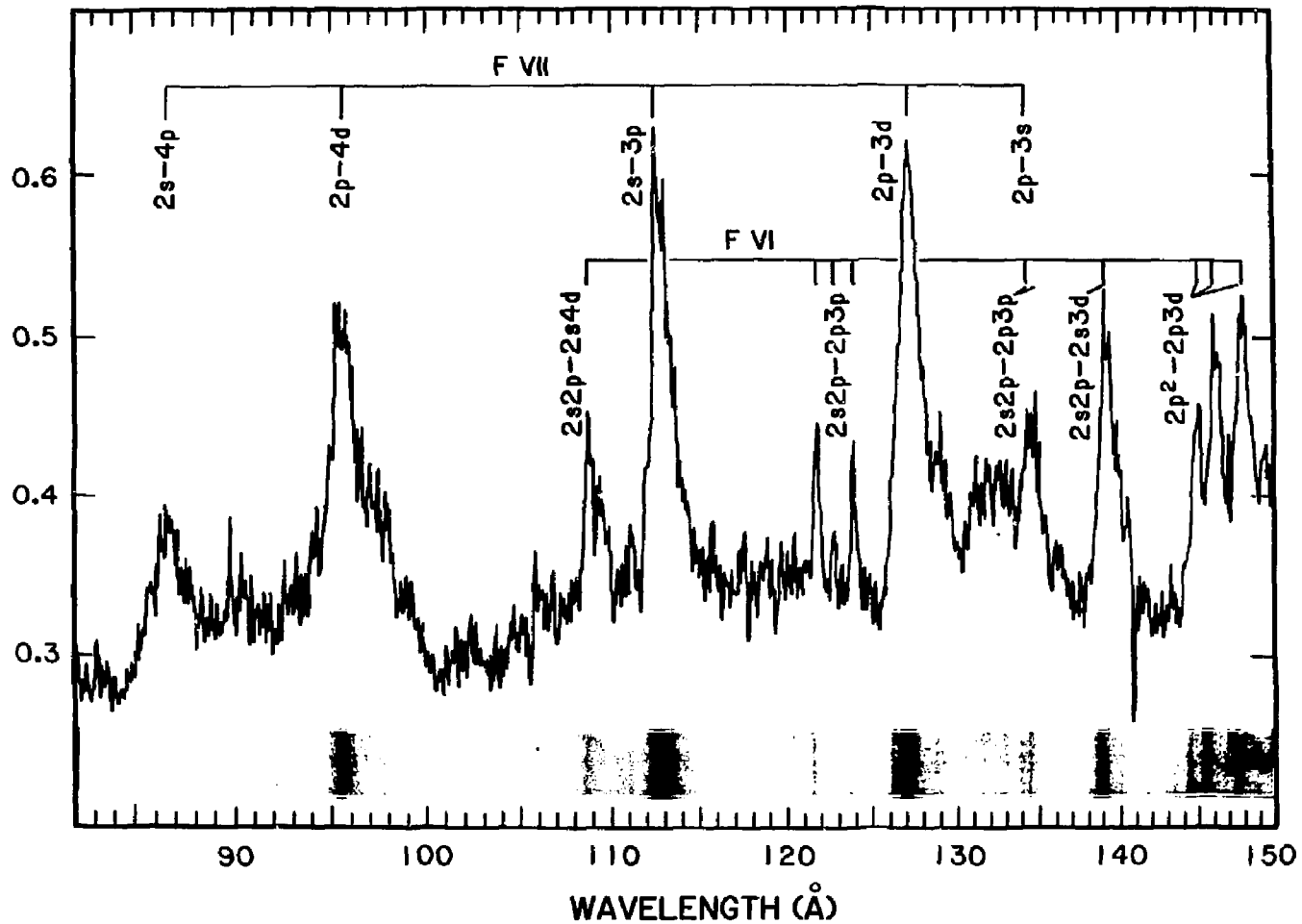
F VII
2s-4p
2p-4d
2s-3p
2p-3d
2p-3s
F VI
2s2p-2s4d
2s2p-2p3p
2s2p-2p3p
2s2p-2s3d
2p²-2p3d
0.6
0.5
0.4
0.3
90
100
110
120
130
140
150
WAVELENGTH (Å)

Fig. 3

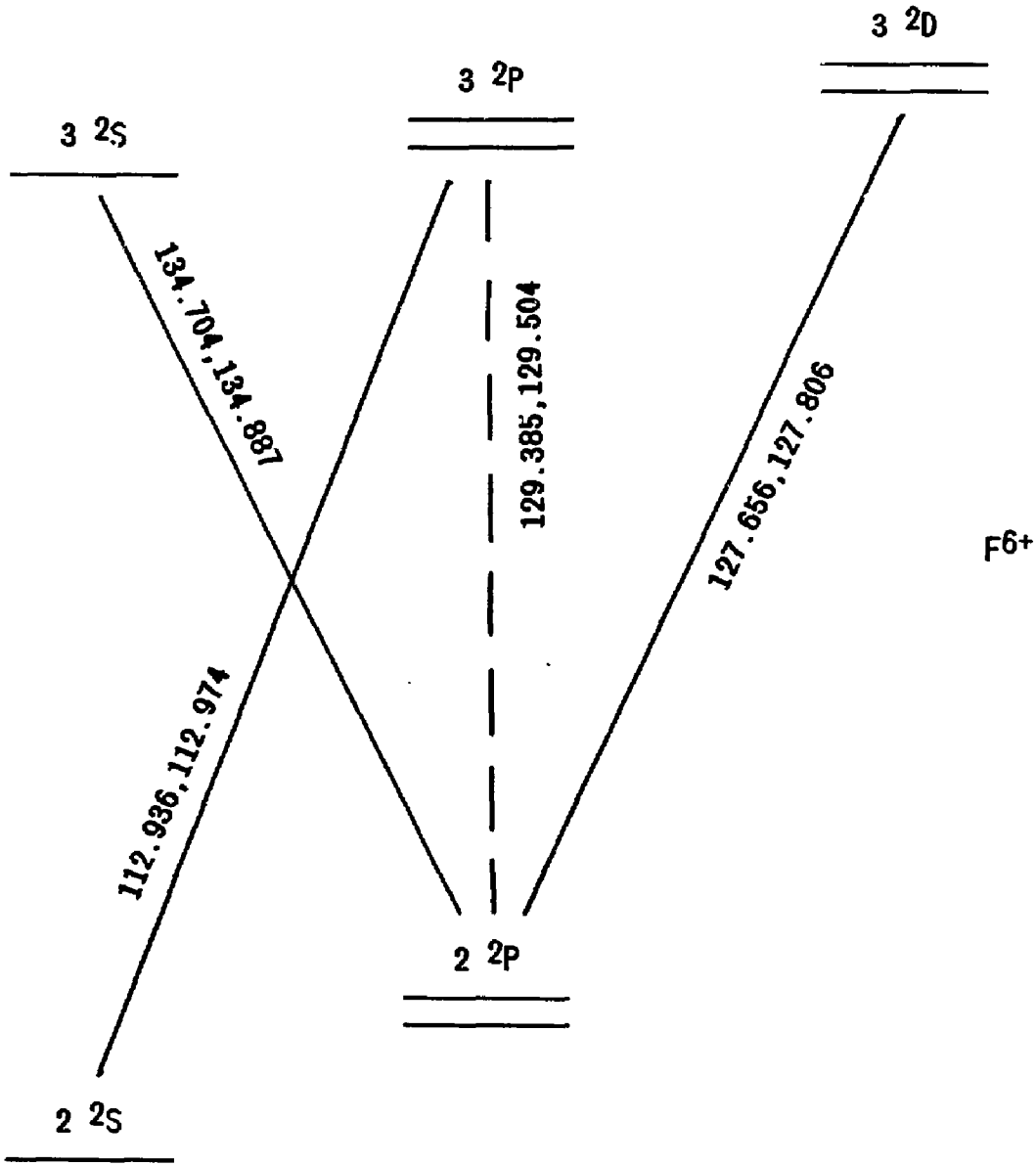
3 2D
3 2P
3 2S
134.704,134.887
129.385,129.504
127.656,127.806
F6+
112.936,112.974
2 2P
2 2S

Fig. 4

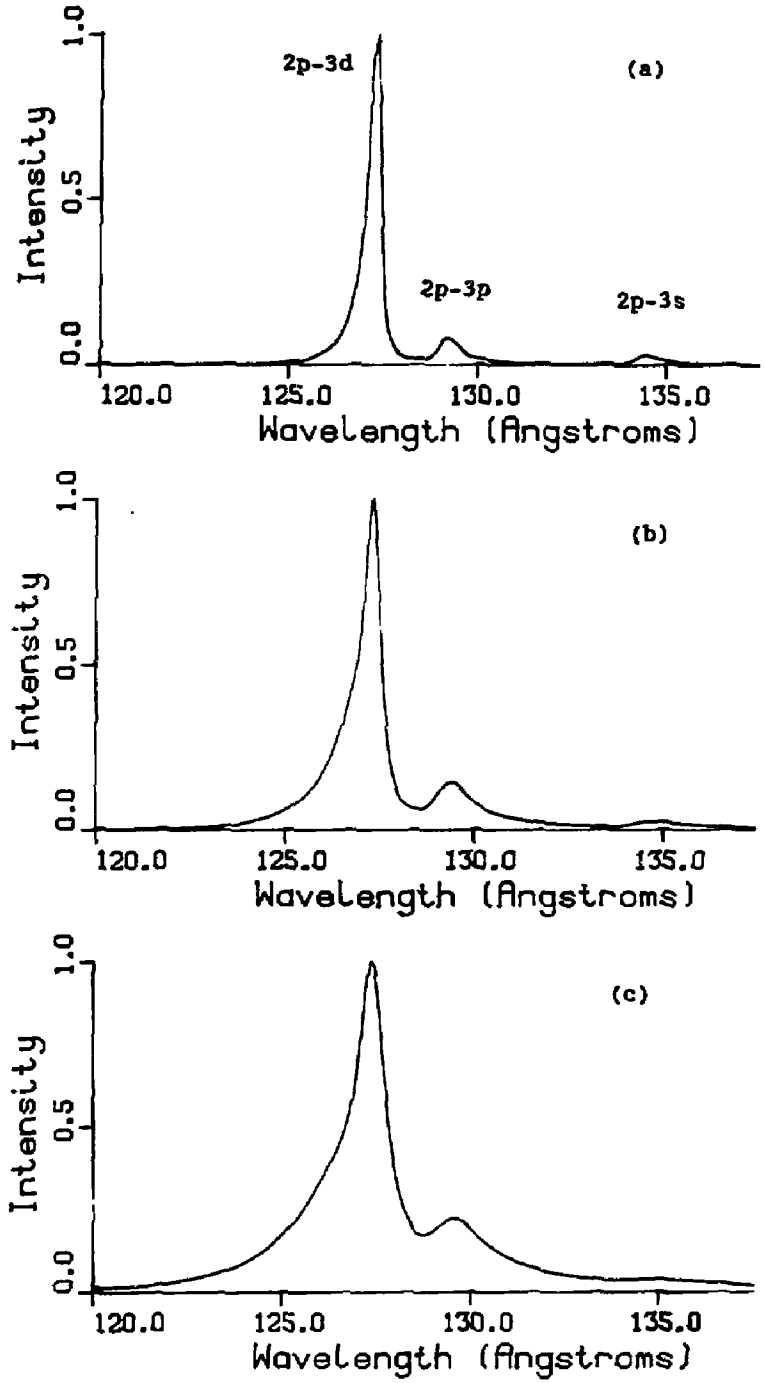
2p-3d
(a)
2p-3p
2p-3s
Intensity
1.0
0.5
0.0
120.0
125.0
130.0
135.0
Wavelength (Angstroms)
(b)
Intensity
1.0
0.5
0.0
120.0
125.0
130.0
135.0
Wavelength (Angstroms)
(c)
Intensity
1.0
0.5
0.0
120.0
125.0
130.0
135.0
Wavelength (Angstroms)

Fig. 5

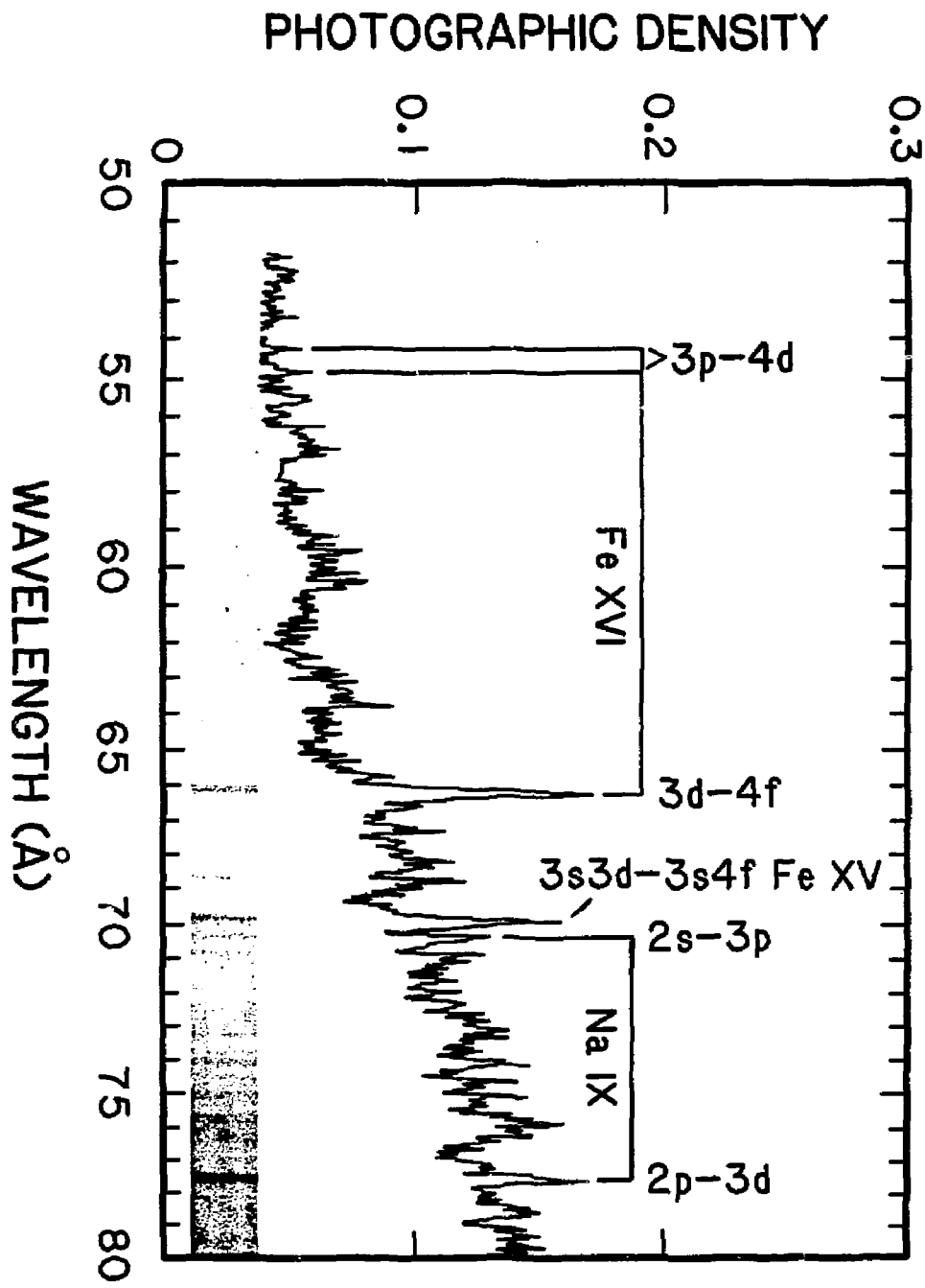
PHOTOGRAPHIC DENSITY
0
0.1
0.2
0.3
WAVELENGTH (Å)
50
55
60
65
70
75
80
>3p-4d
Fe XVI
3d-4f
3s3d-3s4f Fe XV
2s-3p
Na IX
2p-3d

Fig. 6

EXTERNAL DISTRIBUTION IN ADDITION TO UC-20

Dr. Frank J. Paoloni, Univ of Wollongong, AUSTRALIA
Prof. M.H. Brennan, Univ Sydney, AUSTRALIA
Plasma Research Lab., Australian Nat. Univ., AUSTRALIA
Prof. I.R. Jones, Flinders Univ., AUSTRALIA
Prof. F. Cap, Inst Theo Phys, AUSTRIA
Prof. M. Heindler, Institut fur Theoretische Physik, AUSTRIA
M. Goossens, Astronomisch Instituut, BELGIUM
Ecole Royale Militaire, Lab de Phys Plasmas, BELGIUM
Commission-European, Dg-XII Fusion Prog, BELGIUM
Prof. R. Boucique, Laboratorium voor Natuurkunde, BELGIUM
Dr. P.H. Sakanaka, Instituto Fisica, BRAZIL
Instituto De Pesquisas Espaciasi-INPE, BRAZIL
Documents Office, Atomic Energy of Canada Limited, CANADA
Dr. M.P. Bachynski, MPB Technologies, Inc., CANADA
Dr. H.M. Skarsgard, University of Saskatchewan, CANADA
Dr. H. Barnard, University of British Columbia, CANADA
Prof. J. Teichmann, Univ. of Montreal, CANADA
Prof. S.R. Sreenivasan, University of Calgary, CANADA
Prof. Tudor W. Johnston, INRS-Energie, CANADA
Dr. C.R. James, Univ. of Alberta, CANADA
Dr. Peter Lukac, Komenskeho Univ, CZECHOSLOVAKIA
The Librarian, Culham Laboratory, ENGLAND
The Librarian, Rutherford Appleton Laboratory, ENGLAND
Mrs. S.A. Hutchinson, JET Library, ENGLAND
C. Mouttet, Lab. de Physique des Milieux Ionises, FRANCE
J. Radet, CEN/CADARACHE - Bat 506, FRANCE
Univ. of Ioannina, Library of Physics Dept. GREECE
Dr. Tom Mual, Academy Bibliographic Ser., HONG KONG
Preprint Library, Hungarian Academy of Sciences, HUNGARY
Dr. S. Dasgupta, Saha Inst of Nucl. Phys., INDIA
Dr. P. Kaw, Institute for Plasma Research, INDIA
Dr. Philip Rosenau, Israel Inst. Tech, ISRAEL
Librarian, Int'l Ctr Theo Phys, ITALY
Prof. G. Rostagni, Univ Di Padova, ITALY
Miss Clelia De Palo, Assoc EURATOM-ENEA, ITALY
Biblioteca, Instituto di Fisica del Plasma, ITALY
Dr. H. Yamato, Toshiba Res & Dev, JAPAN
Prof. I. Kawakami, Atomic Energy Res. Institute, JAPAN
Prof. Kyoji Nishikawa, Univ of Hiroshima, JAPAN
Direc. Dept. Large Tokamak Res. JAERI, JAPAN
Prof. Satoshi Itoh, Kyushu University, JAPAN
Research Info Center, Nagoya University, JAPAN
Prof. S. Tanaka, Kyoto University, JAPAN
Library, Kyoto University, JAPAN
Prof. Nobuyuki Inoue, University of Tokyo, JAPAN
S. Mori, JAERI, JAPAN
Librarian, Korea Advanced Energy Res. Institute, KOREA
Prof. D.I. Choi, Adv. Inst Sci & Tech, KOREA
Prof. B.S. Liley, University of Waikato, NEW ZEALAND
Institute of Plasma Physics, PEOPLE'S REPUBLIC OF CHINA
Librarian, Institute of Phys., PEOPLE'S REPUBLIC OF CHINA
Library, Tsing Hua University, PEOPLE'S REPUBLIC OF CHINA
Z. Li, Southwest Inst. Physics, PEOPLE'S REPUBLIC OF CHINA
Prof. J.A.C. Cabral, Inst Superior Tecnico, PORTUGAL
Dr. Octavian Petrus, AL I CUZA University, ROMANIA
Dr. Johan de Villiers, Fusion Studies, AEC, SO AFRICA
Prof. M.A. Hellberg, University of Natal, SO AFRICA
C.I.E.M.A.T., Fusion Div. Library, SPAIN
Dr. Lennart Stenflo, University of UMEA, SWEDEN
Library, Royal Inst Tech, SWEDEN
Prof. Hans Wilhelmson, Chalmers Univ Tech, SWEDEN
Centre Phys des Plasmas, Ecole Polytech Fed, SWITZERLAND
Bibliotheek, Fom-Inst Voor Plasma-Fysica, THE NETHERLANDS
Dr. D.D. Ryutov, Siberian Acad Sci, USSR
Dr. G.A. Eliseev, Kurchatov Institute, USSR
Dr. V.A. Glukhikh, Inst Electrophysical Apparatus, USSR
Dr. V.T. Tolok, Inst. Phys. Tech. USSR
Dr. L.M. Kovrizhnykh, Institute Gen. Physics, USSR
Nuclear Res. Establishment, Julich Ltd., W. GERMANY
Bibliothek, Inst. Fur Plasmaforschung, W. GERMANY
Dr. K. Schindler, Ruhr Universitat Bochum, W. GERMANY
ASDEX Reading Rm, IPP/Max-Planck-Institut fur Plasmaphysik, W. GERMANY
Librarian, Max-Planck Institut, W. GERMANY
Prof. R.K. Janev, Inst Phys, YUGOSLAVIA